NIR-I Emissive Cyanine Derived Molecular Probe for Selective Monitoring of the Hepatic Albumin Levels During Hyperglycemic Condition

Bidisha Biswas,[a] Surbhi Dogra,[b] Aniket Sen,[b] N. Arul Murugan, [c] Pooja Dhingra,[a] Kajal Jaswal,[b] Prosenjit Mondal,*[,b,d] Subrata Ghosh *[,a]

[a]*School of Chemical Sciences, Indian Institute of Technology Mandi, Mandi-175001, Himachal Pradesh India.*

[b]*School of Bioscience and Bioengineering, Indian Institute of Technology Mandi, Mandi-175001, Himachal Pradesh India.*

[c]*Department of Computational Biology, Indraprastha Institute of Information Technology, New Delhi, India -110020*

[d]*Department of Biological Sciences, Indian Institute of Science Education and Research Berhampur, Berhampur-760010, India.*

Calculation of quantum yield (Φ):

For determining the quantum yield, IR-125 in ethanol was used as standard.[1] Next, for calculating the quantum yield, the following equation was used,[2,3]

$$\Phi = \frac{A_s F_u n_u^2}{A_u F_s n_s^2} \times \Phi_s$$

A_s= the absorbance value of standard.

A_u= the absorbance value of unknown sample.

F_s = the integrated emission area of standard.

F_u = the integrated emission area of unknown sample.

n_s = the refractive index of the solvent used for standard (corrected to ethanol).

n_u = the refractive index of the solvent used for unknown sample (corrected to be PBS).

Φ_s = the quantum yield of standard (Φ_s=0.132).

Φ_u = the quantum yield of unknown sample.

Dynamic Light Scattering experiment:

The particle sizes for the formation of **BI-CyG** aggregates and the aggregates of **BI-CyG- HSA** complex were investigated using dynamic-light-scattering (DLS) experiment on a Malvern Zetasizer Nano ZS instrument. All the measurements were recorded at ~25 °C in aqueous PBS solutions (pH 7.4).

Determination of the experimental limit of detection:

The experimental limit of detection was calculated following the reported procedure.[4,5] The concentration of albumin at which there was more than 10% of emission intensity enhancement response for **BI-CyG**, compared to the initial emission intensity of **BI-CyG** was considered as the detection limit in this study.

Determination of albumin in serum samples collected from normal volunteer:

Human serum samples collected from normal volunteers have been quantified using BCG method in the pathological lab. The quantified serum sample was then used to prepare serum solutions of different concentrations using serial dilution method. All the prepared samples

were then incubated with the probe (10 μM) for 1 h before subjecting them to fluorescence measurements.

Cell line and culture conditions:

Human hepatocellular carcinoma cell line (HepG2) and human embryonic kidney cell line (HEK293A) were used for all the in vitro experiments. HepG2 cells were maintained in Dulbecco's minimal essential media (DMEM) supplemented with 10% FBS (fetal bovine serum) and 1% penicillin streptomycin (PenStrep) and 293A cells were cultured in DMEM with 10% FBS, 1% non-essential amino acids (NEAA) and 1% PenStrep. The cells were maintained at 37 °C in 5% CO_2.

BI-CyG treatment:

The probe **BI-CyG** was dissolved in DMSO to make a stock of 25 mM concentration. The final concentration utilized for the ensuing experiments was 50 μM. For the in vitro studies, the HepG2 cells following the probe treatment in a serum free media were incubated at 37 ºC for one hour. DMSO was used as vehicle control.

***Invitro* experiments:**

***In vitro* cytotoxicity assay-** The cytotoxicity of **BI-CyG** dye in HepG2 cells was calculated using MTT assay. Towards this, 8000 cells were seeded in a 96-well plate. After 24 hours, cells were treated with the probe **BI-CyG** at different concentrations (12.5, 25, 50, 75, 100 μM) for 24 hours. Thereafter, MTT dye (0.5mg/ml) was added to the cells and incubated for 4 hours. Following this, the media from the cells was removed and the formed formazan crystals were dissolved in DMSO (100 μl). Finally, the absorbance was recorded using iMark plate reader (BIORAD) at 570 nm wavelength. The cell viability was then expressed as percent cell viability relative to control.

siRNA transfection:

HepG2 cells were transfected with albumin siRNA (20 nM) in serum and antibiotic free media on the same day of seeding on the coverslips. After 3 hours, the media was replaced with complete media. **BI-CyG** was treated to the cells post 48 hours of siRNA transfection for one hour. DAPI was used as mounting media to mount the coverslips containing the cells. The images were then visualized using confocal microscopy.

siRNA-albumin

Sense 5'-3' GAAGUUUCCAAGUUAGUGAtt

Antisense 5'-3' UCACUAACUUGGAAACUUCtg

Glucose experimental protocol-

HepG2 cells were seeded onto coverslips at 70% confluence. The following day, cells were first acclimatized to low glucose (5 mM Glucose) for 24 hours. Post treatment in low glucose, the cells were co-treated with high glucose (30 mM glucose) and metformin (1 mM) for 24 hours. The cells were then incubated with 50 µM **BI-CyG** for 1 hour. DMSO was used as vehicle control. Post treatment the cells were washed with PBS and mounted onto slides using DAPI mounting media. The images were recorded using confocal microscopy.

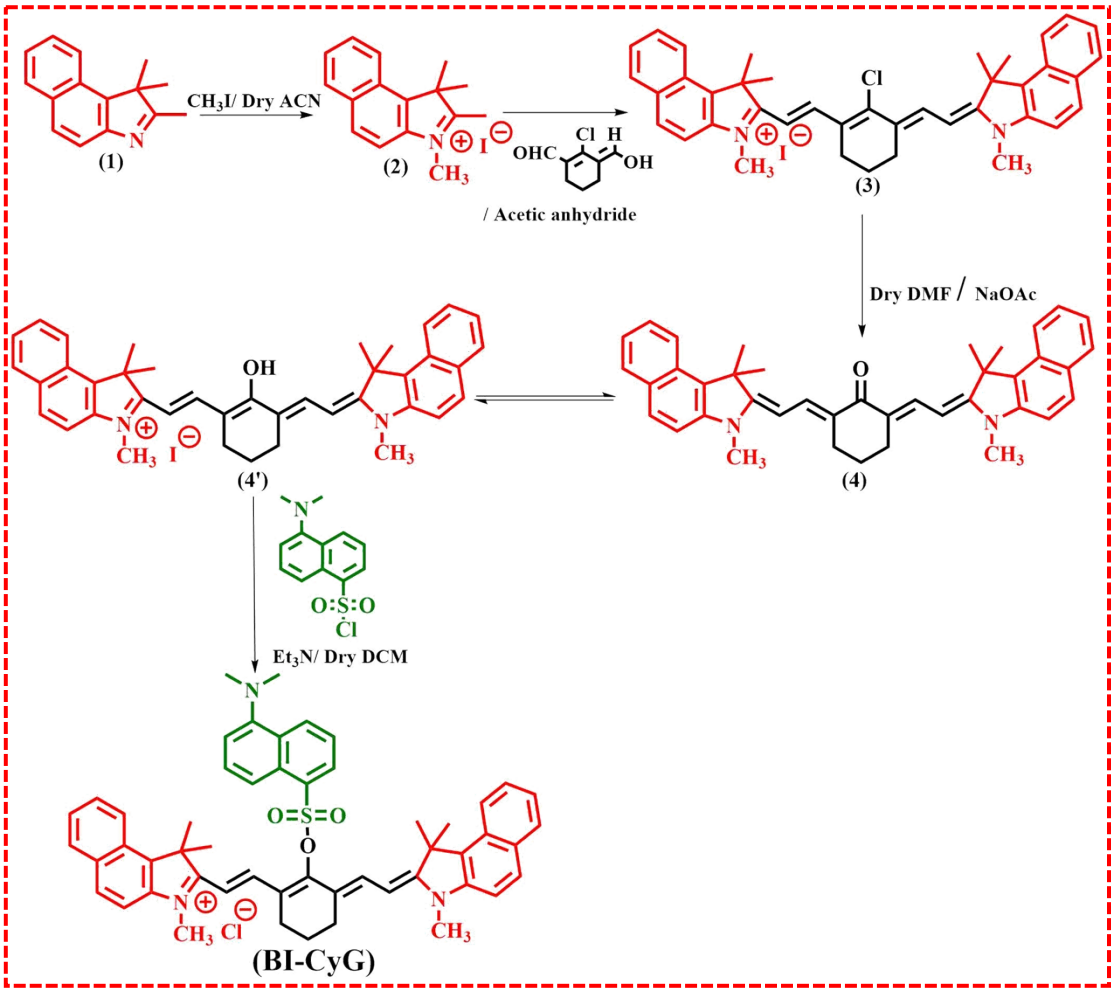

Scheme S1. Synthesis route for **BI-CyG**

Synthesis of intermediates 2-4:

Starting substrate 1 was purchased from commercial source (Sigma-Aldrich). Intermediates 2-4 were synthesized following reported literature methods.[6-8]

Synthesis of BI-CyG-

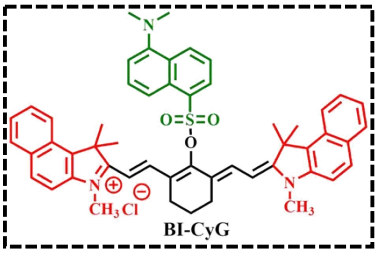

In a dried sealed tube, compound 4′ (1 equivalent) was dissolved in dry DCM under N_2 atmosphere. DABCO (2 equivalent) was added to this resultant solution and was stirred for 15 minutes. To this mixture, dansyl chloride (3 equivalent) was added and left for stirring overnight at 35-37 ºC. After completion of the reaction, the mixture was extracted with water and dichloromethane. The organic layer was collected and dried over sodium sulphate following concentration using rotavapor. The crude green coloured solid was subjected to purification using column chromatography with a mixture of 3%-5% DCM-methanol system as eluent. The product was obtained as deep green solid which was further subjected to ^{1}H-NMR, ^{13}C-NMR, and mass characterization. As evident from literature (particularly from reported NMR spectra) that cyanine probes may trap minor impurities such as grease.

Spectroscopic data of BI-CyG-

^{1}H NMR (500 MHz, $CDCl_3$): δ 8.64 (d, J = 8.25 Hz, 1H), 8.50 (d, J = 8.25 Hz, 1H), 8.29 (d, J = 8.25 Hz, 1H), 7.85 – 7.79 (m, 8H), 7.77 – 7.74 (m, 1H), 7.54- 7.47 (m, 3H), 7.40 – 7.33 (m, 5H), 6.07 (d, J = 14.4 Hz, 2H), 3.70 (s, 6H), 2.95 (s, 6H), 2.68 – 2.66 (m, 4H), 1.95– 1.92 (m, 2H), 1.40 (s, 12H).

^{13}C NMR (125 MHz, $CDCl_3$): δ 173.7, 157.7, 152.3, 140.0, 139.9, 133.7, 132.8, 132.5, 131.8, 130.5, 130.4, 130.1, 129.9, 129.7, 129.6,127.8, 127.5, 124.9, 124.2, 123.6, 121.9, 119.5, 115.9, 110.8, 101.0, 50.6, 45.5, 32.3, 26.6, 25.7, 20.4.

HRMS (ESI): Calc. for $C_{52}H_{52}N_3O_3S$ $[M\text{-}Cl]^+$: 798.3729; Found: 798.3725

Physical Properties: Deep green color solid; **Yield:** 30%

Optical studies with the probe BI-CyG-

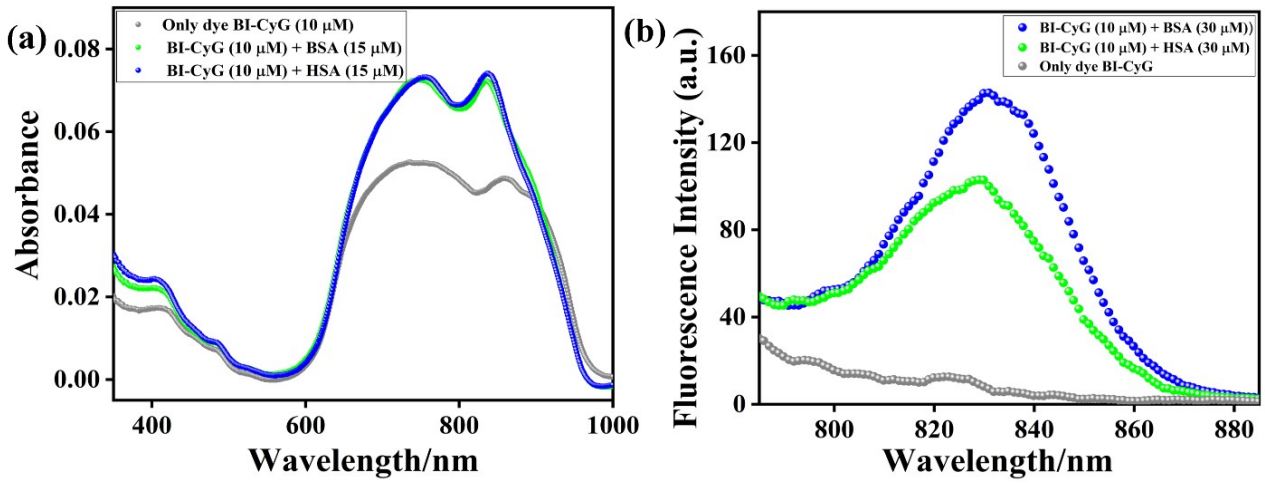

Figure S1. (a) Absorption and (b) emission spectra of **BI-CyG** (10 μM) with/without BSA/HSA (30 μM) in PBS buffer system (10X, pH 7.4)

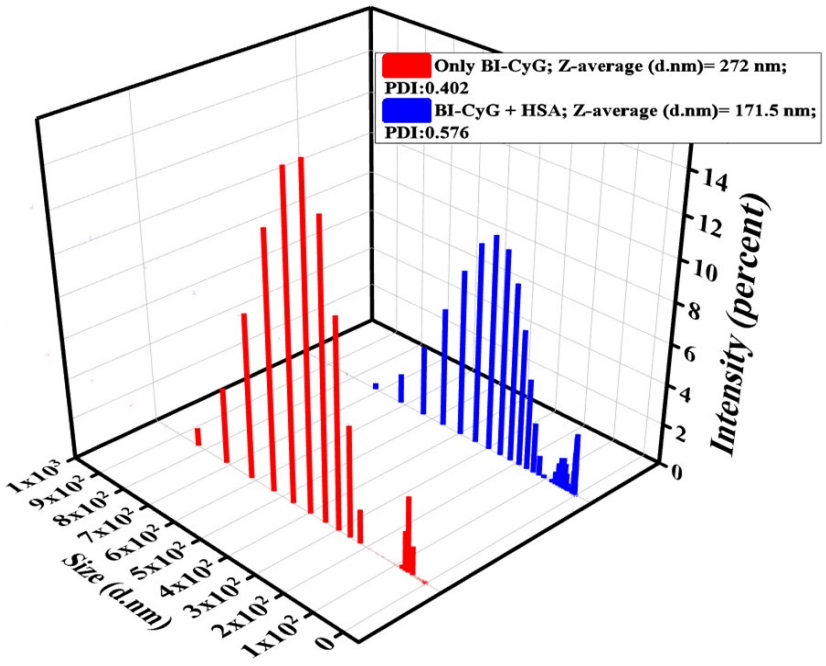

Figure S2. DLS analysis of **BI-CyG** in the absence and upon interaction with HSA.

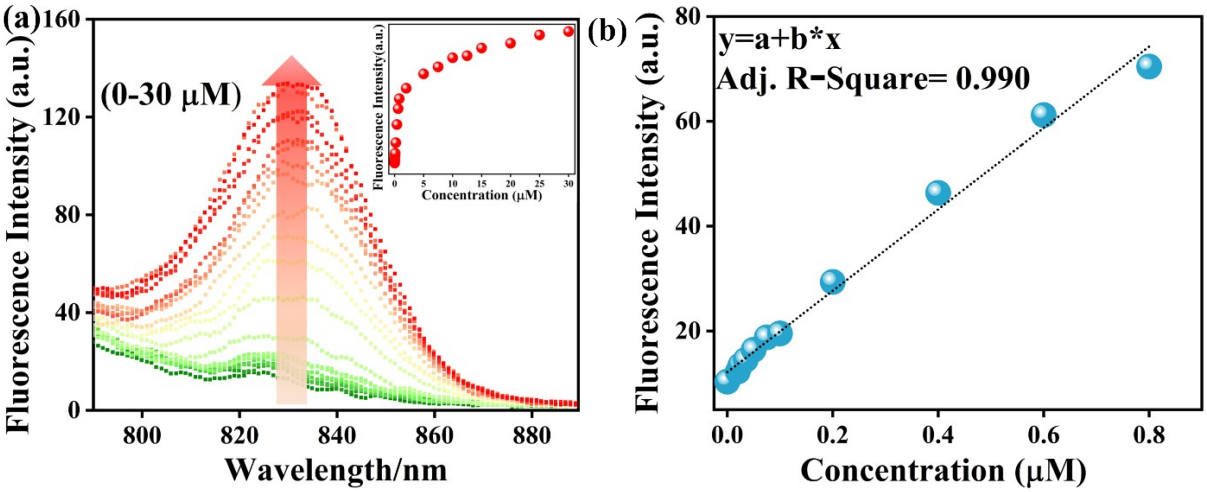

Figure S3. (a) Fluorescence titration spectra of **BI-CyG** (10 μM) with increasing BSA concentrations from 0-30 μM; (b) Linear correlation of **BI-CyG** (10 μM) with the added BSA concentrations in PBS buffer system (10X, pH 7.4).

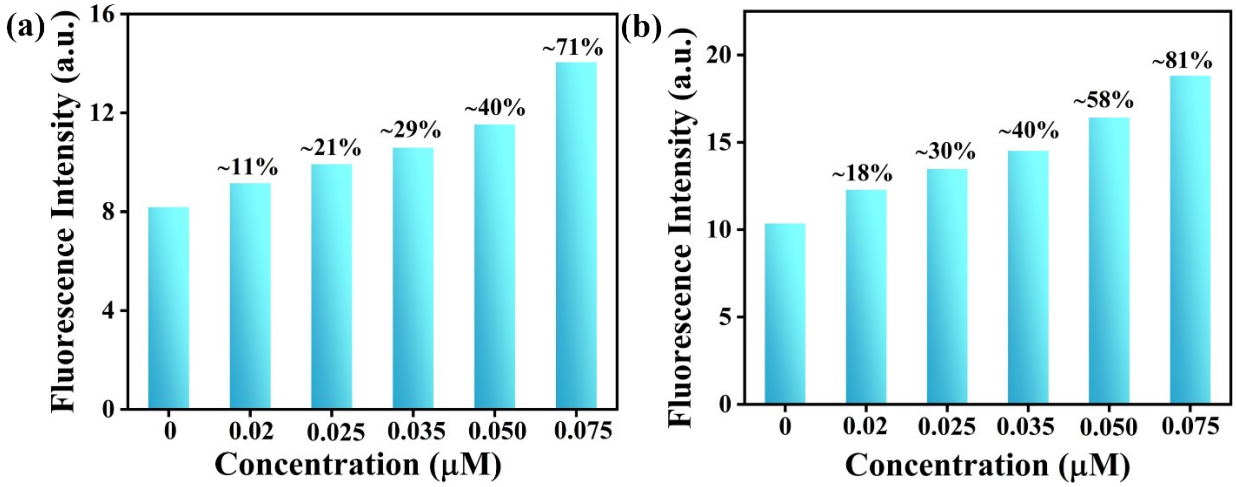

Figure S4. (a) Percentage fluorescence enhancement of **BI-CyG** (10 μM) with incremental addition in the amount of (a) HSA and (b) BSA proteins in PBS buffer system (10X, pH 7.4).

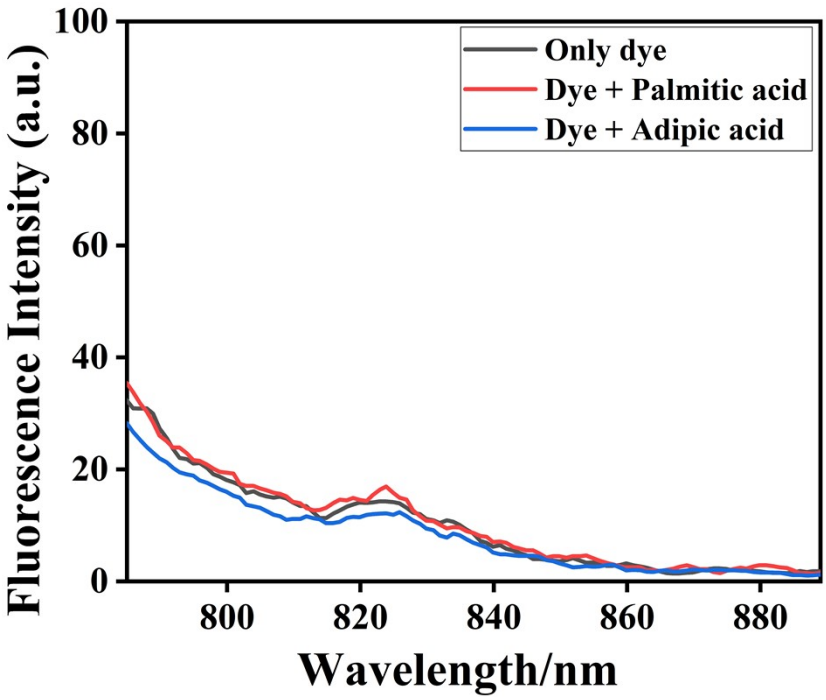

Figure S5. Emission spectra of **BI-CyG** (10 μM) in the presence of different lipids (1 mM) in PBS buffer system (10X, pH 7.4)

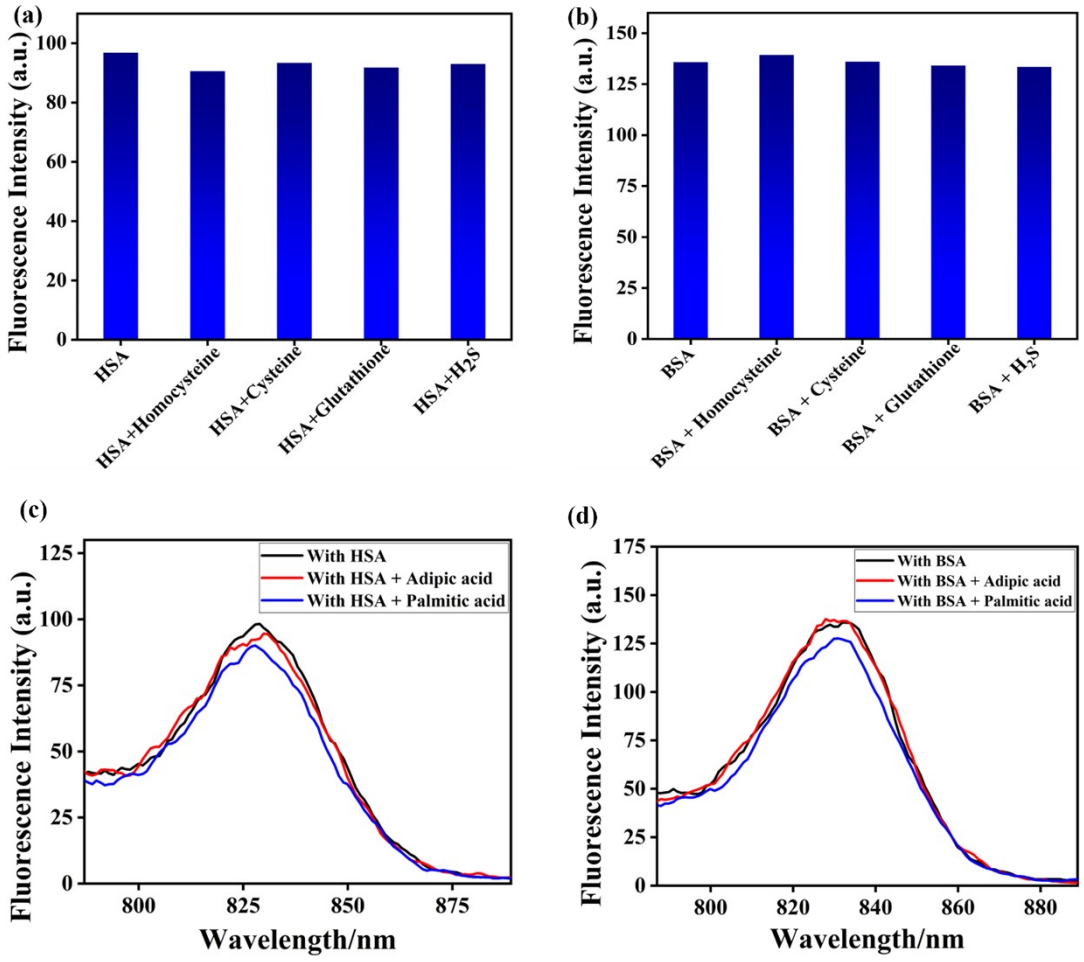

Figure S6. Labelling efficiency of **BI-CyG** (10 µM) towards HSA/BSA in the presence of various (a/b) biothiols (1 mM) and (c/d) fatty acids in PBS buffer system (10X, pH 7.4).

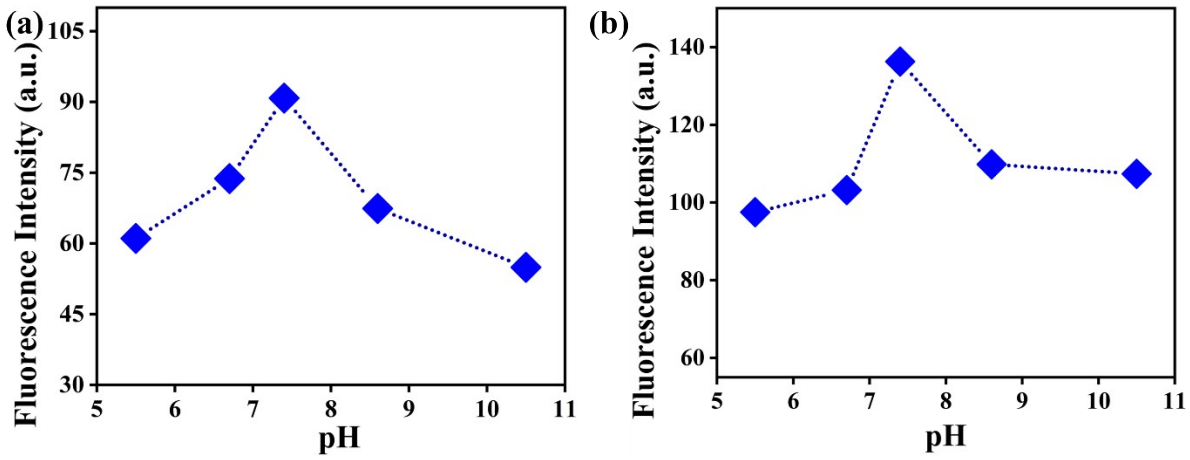

Figure S7. Labelling efficiency of **BI-CyG** (10 µM) towards (a) HSA and (b) BSA in varying pH (5.5- 10.5) in PBS buffer system (10X).

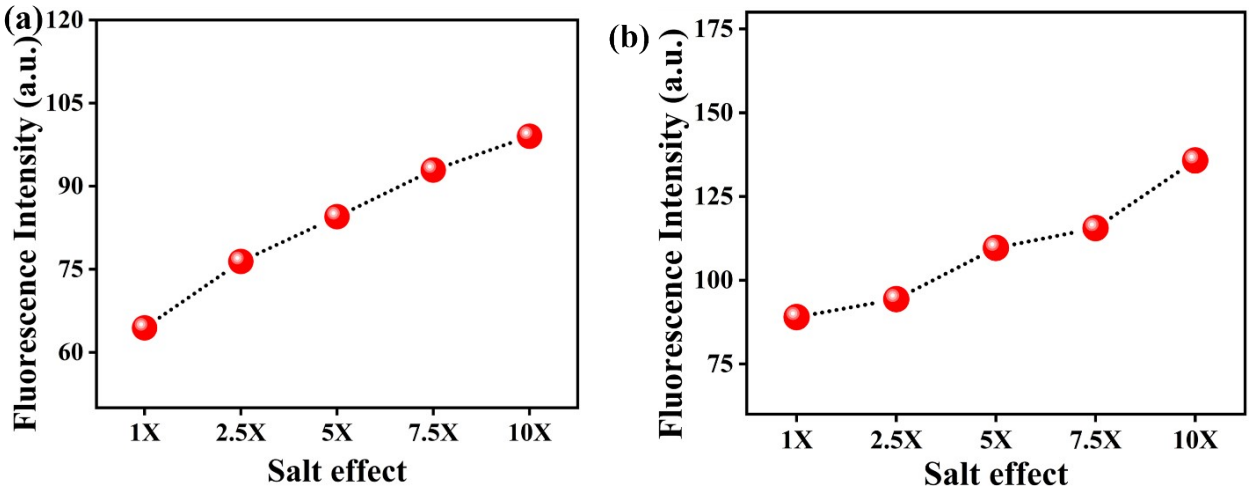

Figure S8. Labelling efficiency of **BI-CyG** (10 µM) towards (a) HSA and (b)BSA in PBS buffer system with varying salt strength from 1X-10X (pH 7.4)

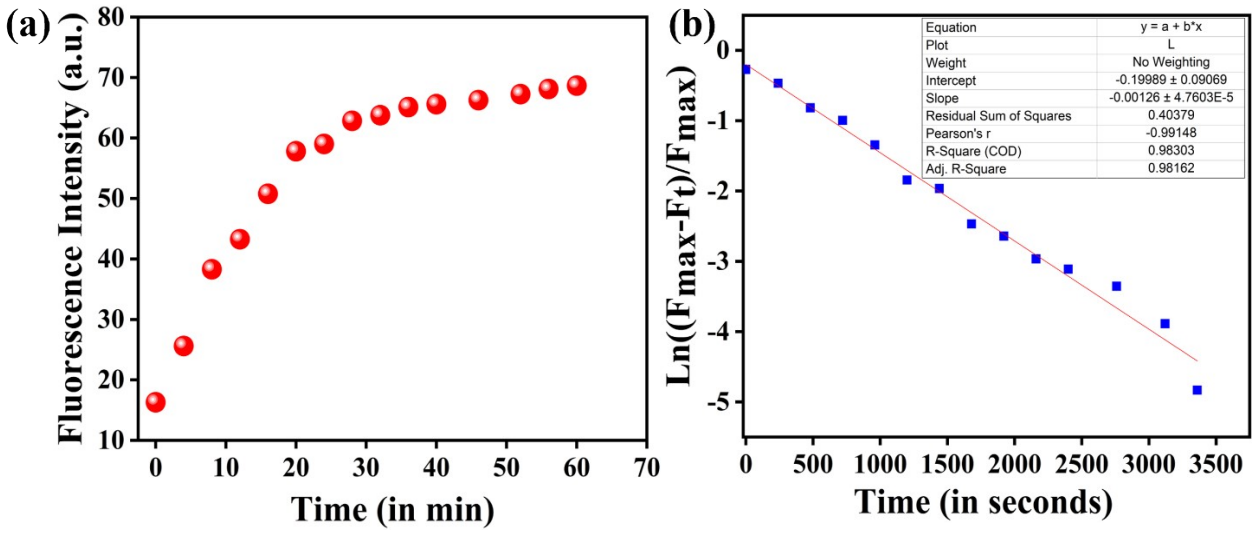

Figure S9. (a) Time dependent emission response of **BI-CyG** (10 μM) in the presence of HSA (30 μM) in PBS buffer system (10X, pH 7.4); (b) Plot of normalized fluorescence intensity of **BI-CyG** (10 μM) with HSA (30 μM) in PBS buffer system (10X, pH 7.4) with time.

Computational tools and studies of BI-CyG-

An integrated approach which includes molecular docking, molecular dynamics and binding free energy calculations has been used to study the conformational dynamics, binding profile and absorption spectra of BI-CYG probe. The molecular docking, molecular dynamics and electronic structure theory calculations were carried out using Autodock4.0, Amber and Gaussian19 software. The binding free energy calculations were carried out using molecular mechanics-Generalized Born surface area (MM-GBSA) approach which is implemented in MMPBSA.py module of AmberTools20 software. The molecular structure of the probe was built using Molden software and the structure was optimized by employing B3LYP/6-31G* level of theory as implemented in Gaussian19 software. The gaussian output file was converted to mol2 and subsequently to pdbqt format using Ambertools and Mgltools respectively. The pdbqt file provides information about the number of torsional bonds and the charges for all the

atoms which are used in the docking energy calculation by the Autodock software. The 3D structure for carrying out molecular dynamics has been downloaded from protein databank and the PDB id for the structure used is 1AO6 (the resolution is reported to be 2.5 Å which suggests that the structure is reasonably accurate). In particular, the HSA is known to have multiple binding sites and as the binding site for the probe is not known, we have carried out a blind docking by choosing a grid box which can include the whole protein. The grid size used is 0.375 Å which is the default value set in the software. The number of grid points along x, y and z directions are 130, 130 and 160. The Lamarckian genetic algorithm has been used for finding the most stable binding modes of probe in the HSA. The algorithm treats different degrees of freedom of the probe as a gene and sampling over them is performed by doing a number of operations such as mutation, cross over and selection. We have also identified multiple binding sites for the probe within the HSA and we have considered the top binding sites of the probe for further exploration using molecular dynamics and free energy calculations approach. The charges for the probe were obtained by carrying out the single point calculation by employing B3LYP/6-31G* level of theory. The charges were computed using pop=MK procedure which provides the charges that can reproduce the molecular electrostatic potential at number of grid points located on different layers around the molecule. The interaction has been described using general amber force-field. For the HSA we used FF19SB force field. Based on the docking results a complex structure with protein and probes bound in different sites of protein has been prepared. The ligands in top three binding sites were used for the preparation of the complex structure. The complex has been solvated with approximately 40000 water molecules. The Na+ ions were added to neutralize the whole protein-ligand system. The molecular dynamics in isothermal-isobaric ensemble has been carried out for a total time scale of 100 ns. The production run has been carried out followed by a minimization run (usually carried out to remove any hot spots in the input structure), simulation in constant

volume ensemble. Further an equilibration run for a time scale of 10 ns as well carried out to allow the system to equilibrate before the production run is initiated. The time step for the integration of equation of motion was 2 fs. The binding free energy calculations were carried out using the trajectory corresponding to last 10 ns in the production run. In particular, 1000 configurations were used to compute the binding free energies using MM-GBSA approach which is implemented in the MMPBSA.py module of the Ambertools. The rmsd of the ligand and its conformational dynamics in different binding sites were analysed using cpptraj module of Ambertools**.**

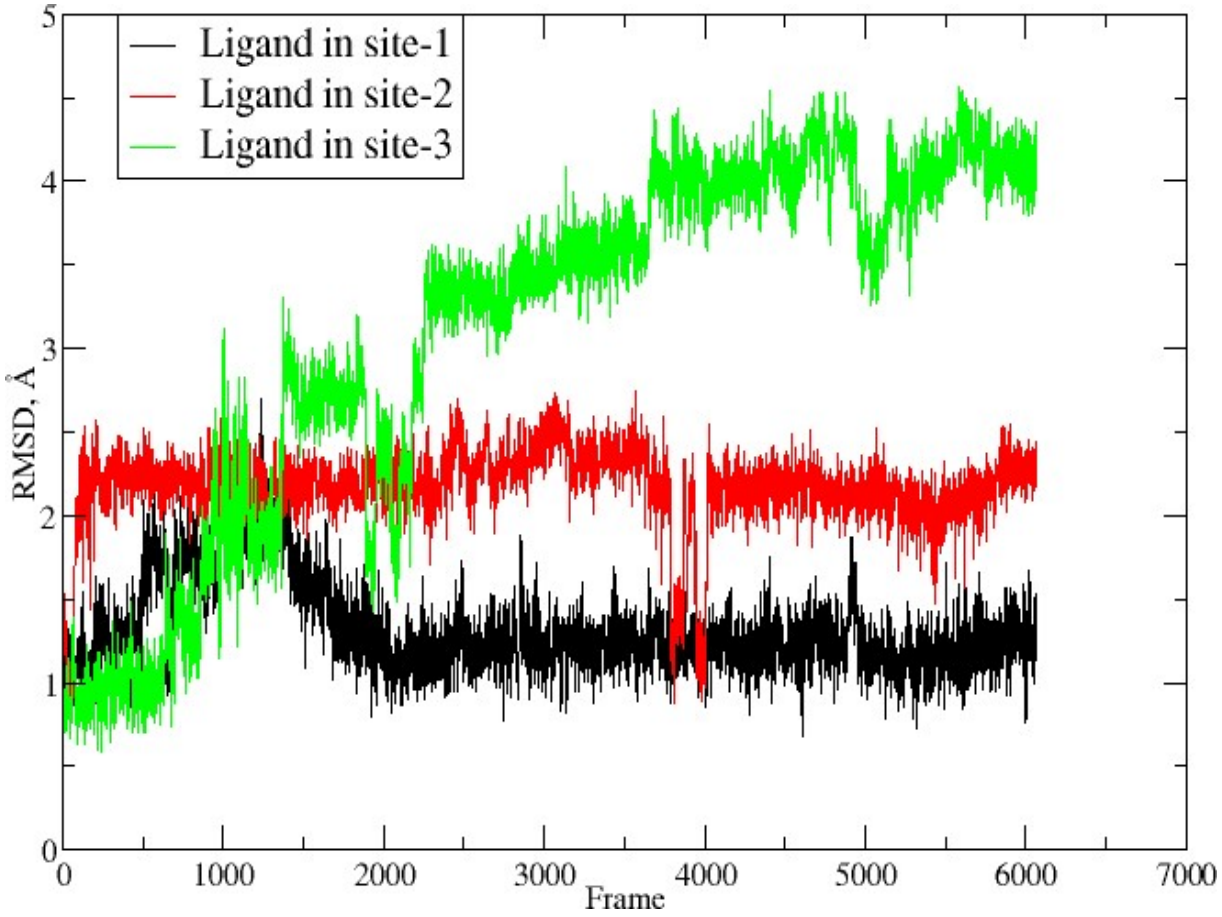

Figure S10. The time evolution of RMSD for **BI-CyG** in the different binding sites.

Table S1: The binding free energy of the probe **BI-CyG** with HSA protein and different contributions.

Site	Evdw	Eelec	Epol solvation	Enp solvation	ΔG, kcal/mol
Site-1	-70.70	-68.07	114.51	-8.26	**-32.49**
Site-2	-63.51	-206.02	238.85	-7.24	**-37.90**
Site-3	-70.47	-176.40	219.64	-8.64	**-35.85**

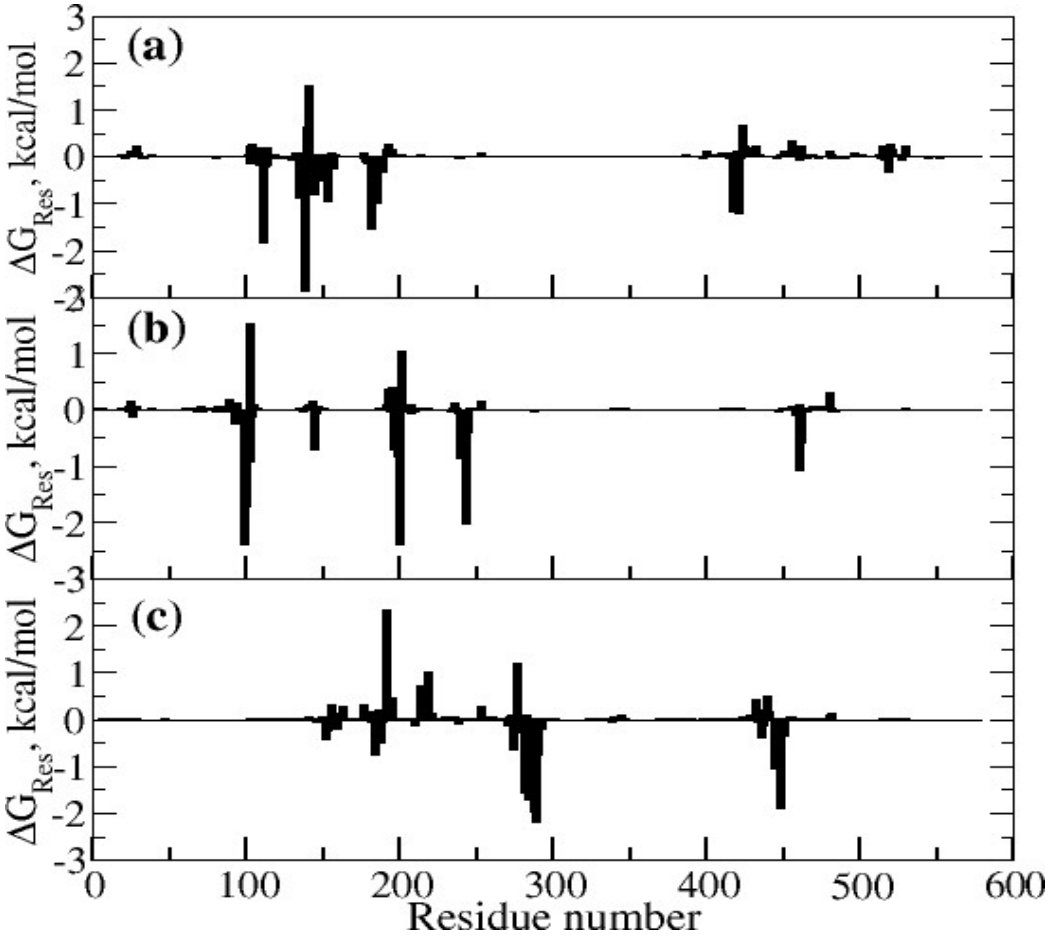

Figure S11. Free energy decomposition analysis for **BI-CyG** in the binding sites (a) 1, (b) 2 and (c) 3 respectively.

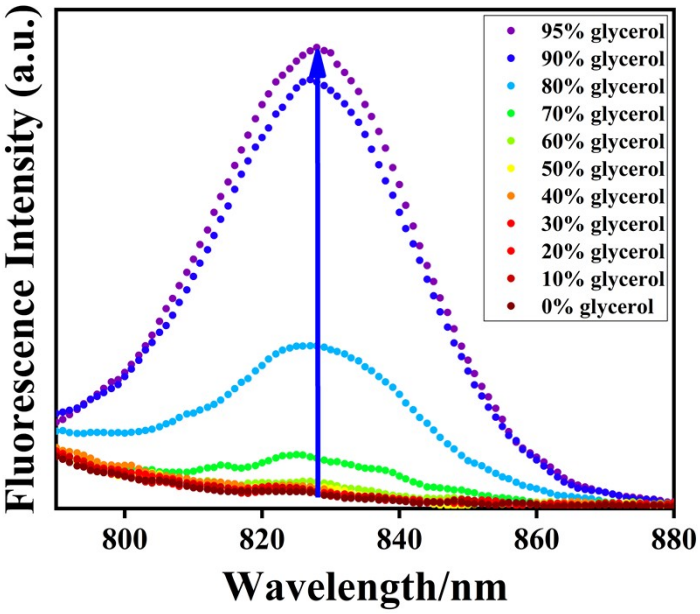

Figure S12. Fluorescence response of **BI-CyG** with increasing viscosity of the water-glycerol medium (glycerol 0-95%)

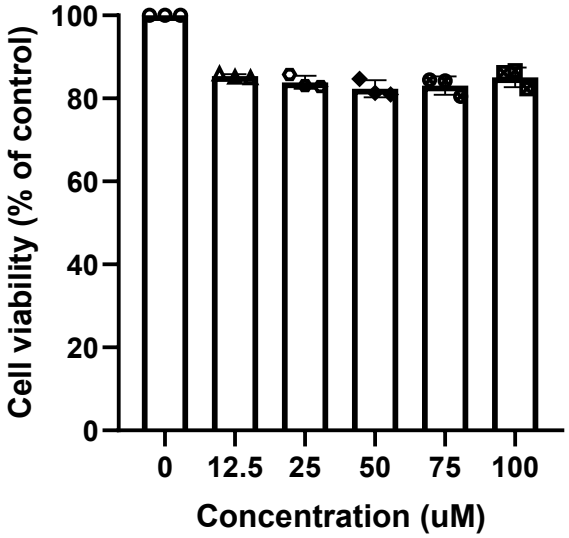

Figure S13. Cell viabilities of HepG2 cells treated with different concentrations (0–100 μM) of **BI-CyG** (recorded after 24 h).

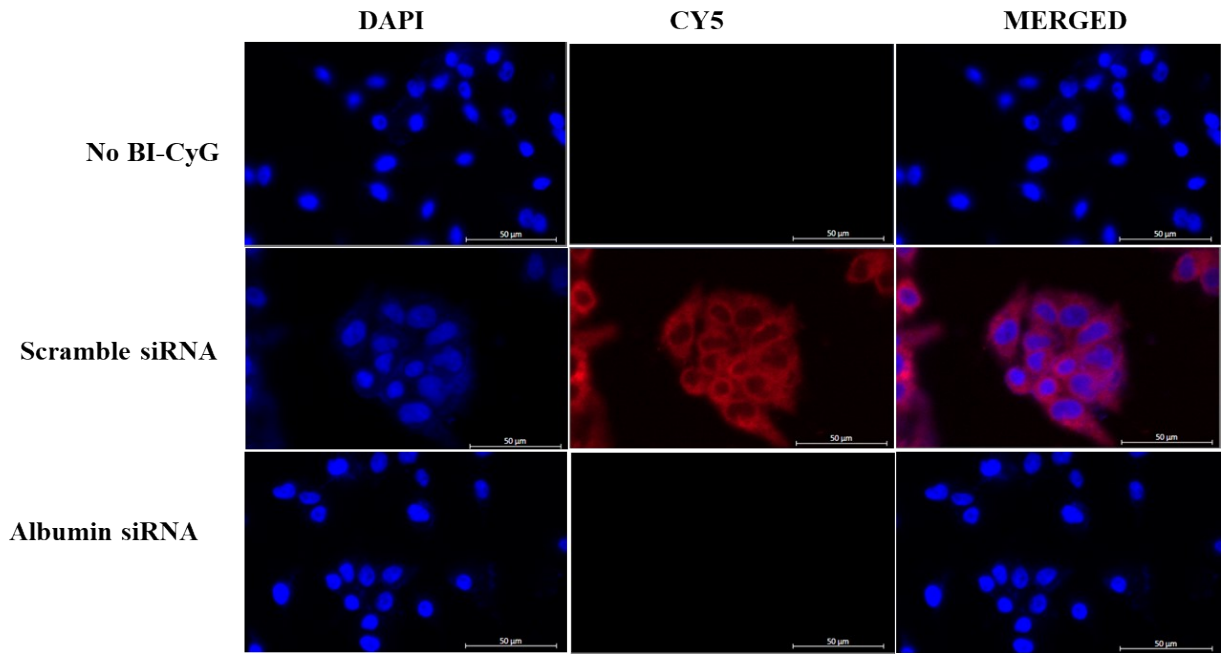

Figure S14. The siRNA-mediated knockdown of albumin and subsequent visualization using **BI-CyG**. Treatment of HepG2 cells with albumin−siRNA (20 nM) and scramble siRNA (20 nM) (in control cells) for 48 h, followed by incubation with **BI-CyG** for 1 h, and finally visualization under a confocal microscope.

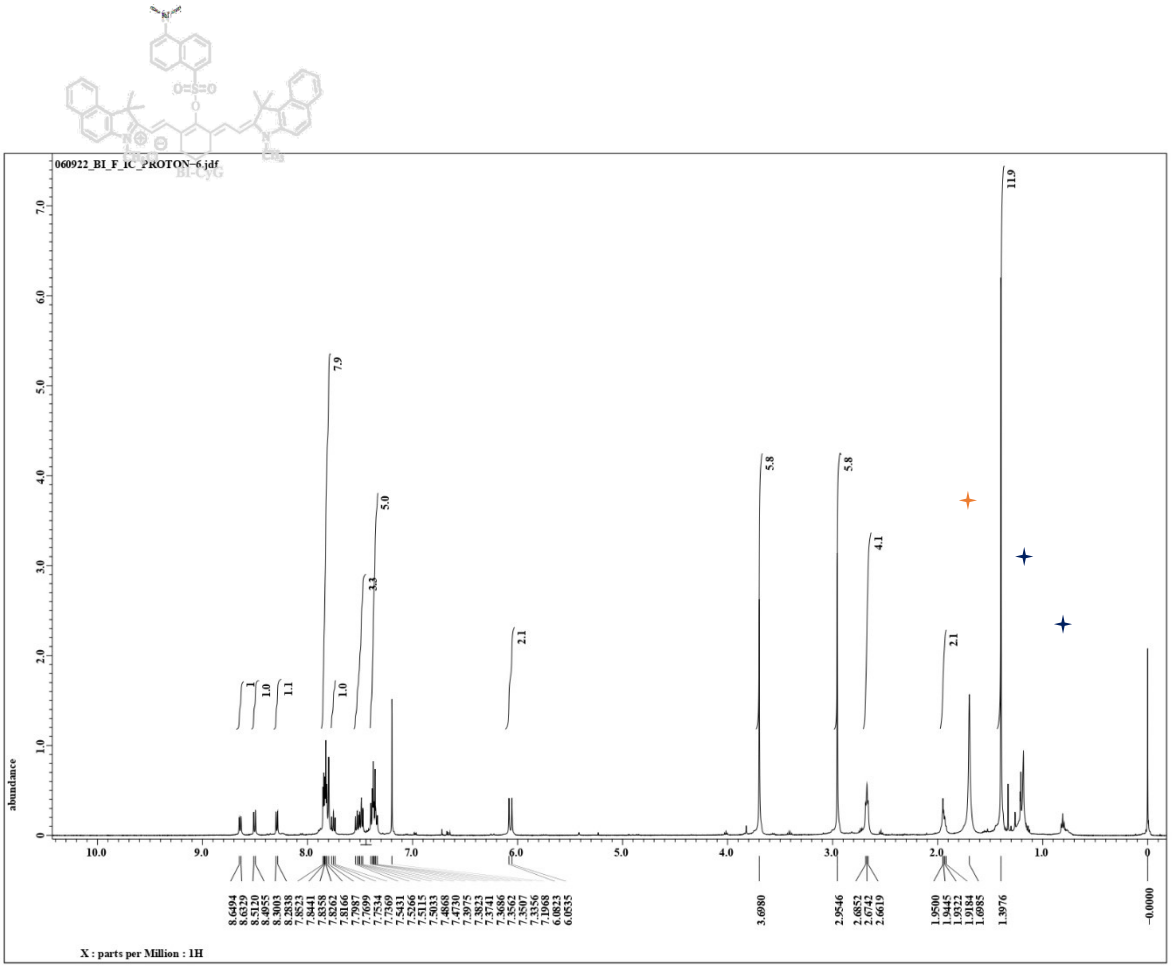

✦ Grease peaks; ✦ water peak

Figure S15. ^{1}H NMR spectrum of **BI-CyG**.

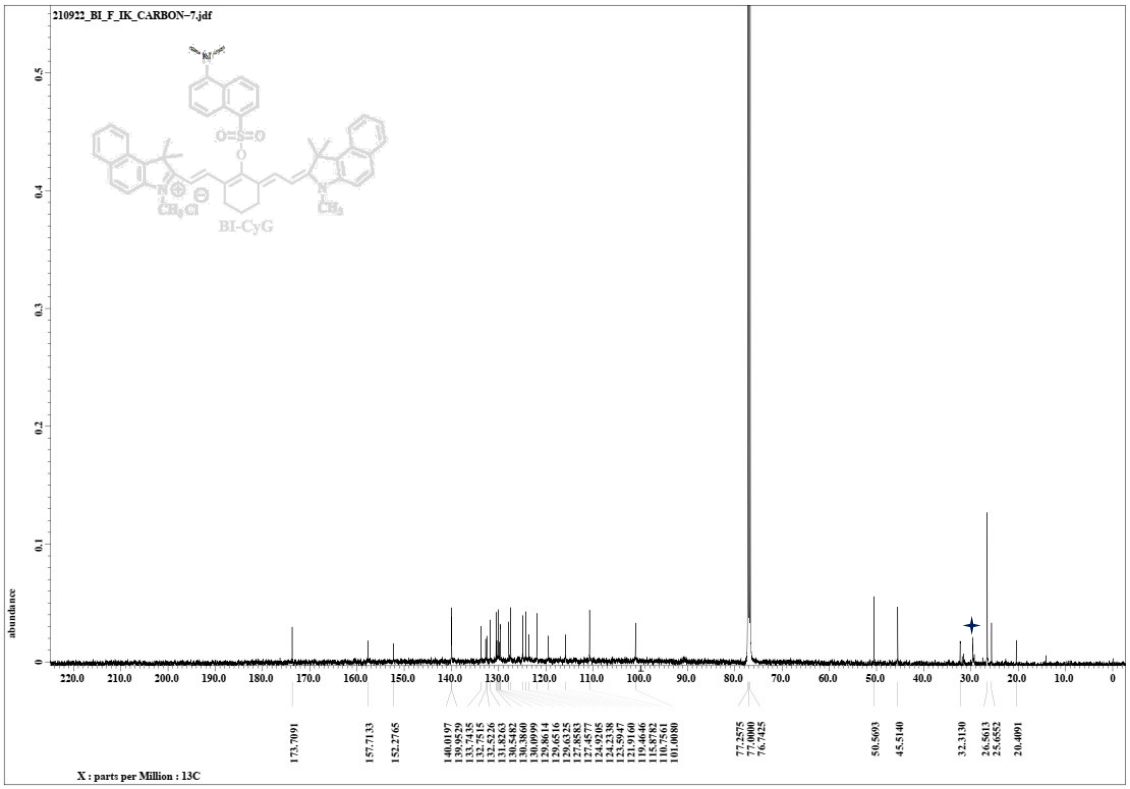

✦ Grease peak

Figure S16. ^{13}C NMR spectrum of **BI-CyG**.

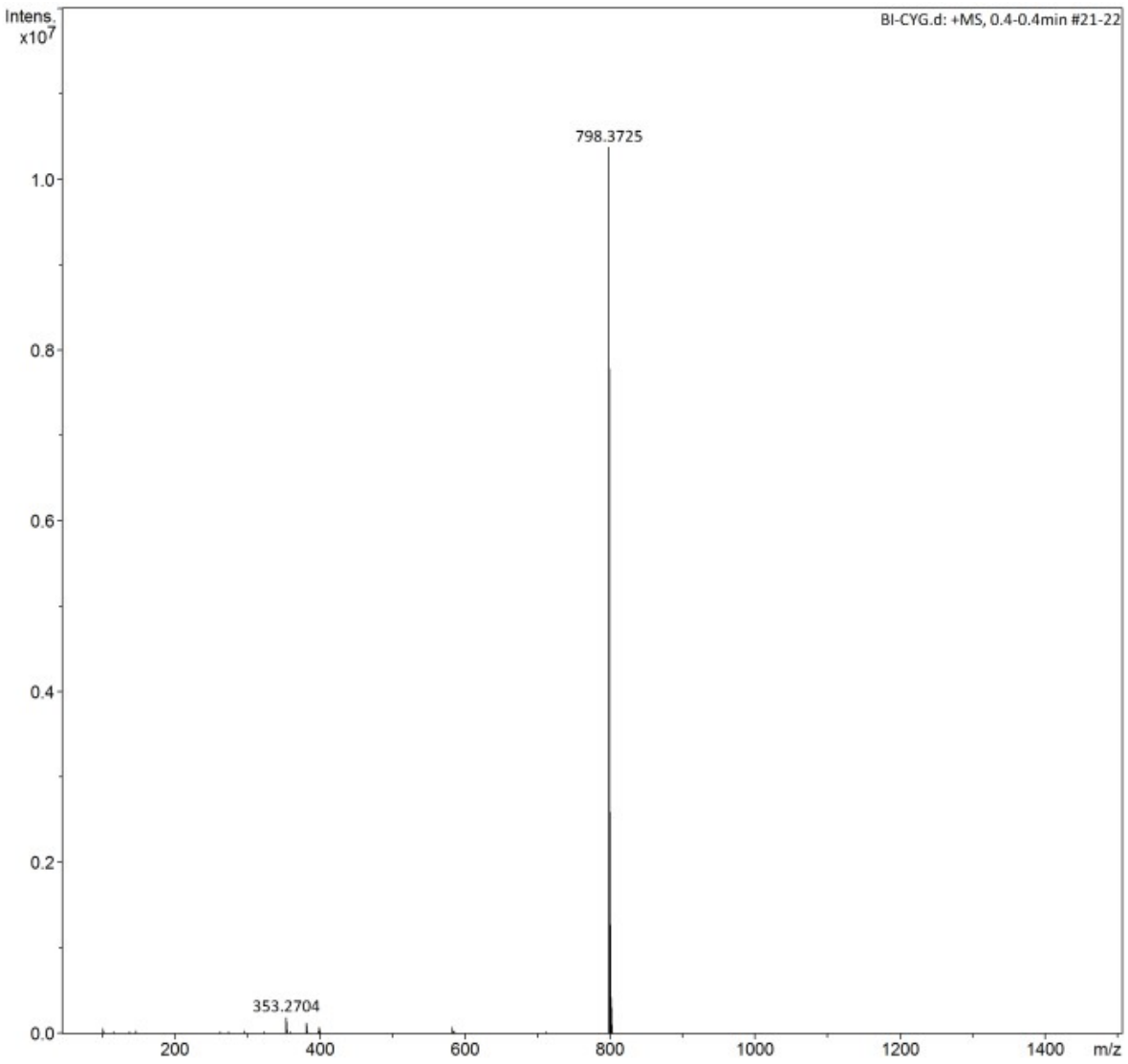

Figure 17. HRMS spectra of **BI-CyG**.

References

1. K. Rurack, M. Spieles, Fluorescence quantum yields of a series of red and near-infrared dyes emitting at 600− 1000 nm, *Anal. Chem.* 2011, **83**, 1232-1242.

2. C. Würth, M. Grabolle, J. Pauli, M. Spieles, U. Resch-Genger, Relative and absolute determination of fluorescence quantum yields of transparent samples, *Nat. Protoc.* 2013, **8**, 1535-1550.

3. D.F. Eaton, Reference materials for fluorescence measurement, *Pure Appl. Chem.* 1988, **60**, 1107-1114.

4. B. Liu, Y. Pang, R. Bouhenni, E. Duah, S. Paruchuri, L. McDonald, A step toward simplified detection of serum albumin on SDS-PAGE using an environment-sensitive flavone sensor, *Chem. Commun.* **2015**, 51, 11060-11063.

5. T. Jin, Near-infrared fluorescence detection of acetylcholine in aqueous solution using a complex of rhodamine 800 and *p*-sulfonato-calix[8]arene, *Sensors*, 2010, **10**, 24382449.

6. X. Wang, Z. Guo, S. Zhu, H. Tian, W. Zhu, A naked-eye and ratiometric near-infrared probe for palladium via modulation of a π-conjugated system of cyanines, *Chem. Commun.* 2014, **50**, 13525-13528.

7. Y. Li, Y. Sun, J. Li, Q. Su, W. Yuan, Y. Dai, C. Han, Q. Wang, W. Feng, F. Li, Ultrasensitive near-infrared fluorescence-enhanced probe for in vivo nitroreductase imaging, *J. Am. Chem. Soc.* 2015, **137**, 6407-6416.

8. C. Hu, W. Sun, J. Cao, P. Gao, J. Wang, J. Fan, F. Song, S. Sun, X. Peng, A ratiometric near-infrared fluorescent probe for hydrazine and its in vivo applications, *Org. Lett.* 2013, **15**, 4022-4025.